Journal of Applied Mechanics and Technical Physics, Vol. 48, No. 2, pp. 221–228, 2007

FORCED OSCILLATIONS OF A LAYER OF A VISCOELASTIC MATERIAL UNDER THE ACTION OF A CONVECTIVE PRESSURE WAVE

V. M. Kulik

UDC 532.591; 539.3.371

The longitudinal and transverse components of deformation of the surface of a flat layer of a viscoelastic material glued onto a solid base under the action of a traveling pressure wave are determined. The coating compliance is described by two components corresponding to two components of surface displacement. The dimensionless compliance components depend only on the viscoelastic properties of the material, the ratio of the wave length to the layer thickness λ/H, and the ratio of the wave velocity to the velocity of propagation of shear oscillations V/C_t^0. Data on the dynamic compliance are presented for $0.3 < \lambda/H < 30$ and $0.1 < V/C_t^0 < 10$. The compliance is demonstrated to be determined by its absolute value and by the phase lag of strain from pressure. The effect of viscous losses in the material and compressibility of the latter on the dynamic compliance is analyzed. An anomalous behavior of the compliance with the wave velocity being greater than a certain critical value is explained.

Key words: *forced oscillations, elasticity modulus, loss factor, Poisson's ratio, dynamic compliance.*

The complex compliance of a layer of a viscoelastic material of thickness H with Poisson's ratio σ, density ρ, and complex elasticity modulus $E^* = E(1 - i\mu)$ (μ is the loss factor), which is glued to a solid base, is calculated in the present paper. A steady regime of deformation of this coating under the action of a plane monochromatic pressure wave propagating along the x axis with a velocity V is considered.

The displacement of particles of the medium is described by the dependence

$$\boldsymbol{\xi} = \boldsymbol{i}\zeta + \boldsymbol{j}\eta = \boldsymbol{f}(y)\,\mathrm{e}^{i\omega(x/V-t)},$$

where ζ and η are the displacement components directed along the coating and perpendicular to it, respectively.

The global equation of motion has the form [1]

$$\frac{\partial^2 \boldsymbol{\xi}}{\partial t^2} = C_t^2 \Delta \boldsymbol{\xi} + (C_l^2 - C_t^2)\,\mathrm{grad}\,\mathrm{div}\,\boldsymbol{\xi}, \tag{1}$$

where $C_l = [E^*(1-\sigma)/(\rho(1+\sigma)(1-2\sigma))]^{1/2}$ is the velocity of the compression-extension wave in an infinite space and $C_t = [E^*/(2\rho(1+\sigma))]^{1/2}$ is the velocity of the shear wave in an infinite space.

The boundary conditions are the condition of the absence of displacements on the solid wall

$$\zeta = \eta = 0 \qquad \text{for} \quad y = H \tag{2}$$

and the condition of identical stresses on the external boundary

$$C_l^2 \frac{\partial \eta}{\partial y} + (C_l^2 - 2C_t^2)\frac{\partial \zeta}{\partial x} = -\frac{P}{\rho}\,\mathrm{e}^{i\omega(x/V-t)}, \qquad \frac{\partial \zeta}{\partial y} + \frac{\partial \eta}{\partial x} = 0 \qquad \text{for} \quad y = 0. \tag{3}$$

Kutateladze Institute of Thermophysics, Siberian Division, Russian Academy of Sciences, Novosibirsk 630090; kulik@itp.nsc.ru. Translated from Prikladnaya Mekhanika i Tekhnicheskaya Fizika, Vol. 48, No. 2, pp. 90–97, March–April, 2007. Original article submitted February 1, 2006; revision submitted April 24, 2006.

0021-8944/07/4802-0221

Equation (1) is solved by the method of displacement division into the gradient and rotor parts. We introduce two scalar functions Φ and Ψ such that

$$\zeta = \frac{\partial \Phi}{\partial x} + \frac{\partial \Psi}{\partial y}, \qquad \eta = \frac{\partial \Phi}{\partial y} - \frac{\partial \Psi}{\partial x}. \tag{4}$$

Substituting them into Eq. (1), we obtain the equations

$$\frac{\partial^2 \Phi}{\partial t^2} - C_l^2 \Delta \Phi = 0, \qquad \frac{\partial^2 \Psi}{\partial t^2} - C_t^2 \Delta \Psi = 0,$$

whose solution has the form

$$\Phi = \Big[A_1 \frac{\sinh\,(\omega\alpha y/V)}{\omega\alpha/V} + B_1 \cosh\,(\omega\alpha y/V) \Big] \mathrm{e}^{i\omega(x/V-t)},$$

$$\Psi = \Big[A_2 \frac{\sinh\,(\omega\beta y/V)}{\omega\beta/V} + B_2 \cosh\,(\omega\beta y/V) \Big] \mathrm{e}^{i\omega(x/V-t)}.$$

Here $\alpha = [1 - (V/C_l)^2]^{1/2}$ and $\beta = [1 - (V/C_t)^2]^{1/2}$.

Using the boundary conditions (2) and (3), we obtain a system of four equations for A_1, A_2, B_1, and B_2:

$$A_1 = -\frac{\alpha(1+\beta^2)F}{1+\beta^2-2S} \frac{\lambda P}{4\pi\rho C_t^2}, \qquad A_2 = \frac{iS}{1+\beta^2-2S} \frac{\lambda P}{2\pi\rho C_t^2},$$

$$B_1 = -\frac{1}{1+\beta^2-2S} \frac{\lambda^2 P}{4\pi^2\rho C_t^2}, \qquad B_2 = \frac{i\alpha F}{1+\beta^2-2S} \frac{\lambda^2 P}{4\pi^2\rho C_t^2}.$$

Here

$$S = (\cosh\,(2\pi\alpha H/\lambda) - \alpha\beta DF)/\cosh\,(2\pi\beta H/\lambda),$$

$$F = \frac{\sinh\,(2\pi\alpha H/\lambda) - (\alpha\beta)^{-1}\cosh\,(2\pi\alpha H/\lambda)\tanh\,(2\pi\beta H/\lambda)}{\cosh\,(2\pi\beta H/\lambda) - ((1+\beta^2)/2)\cosh\,(2\pi\alpha H/\lambda) - D\tanh\,(2\pi\beta H/\lambda)},$$

$$D = \sinh\,(2\pi\beta H/\lambda) - ((1+\beta^2)/(2\alpha\beta))\sinh\,(2\pi\alpha H/\lambda),$$

and $\lambda = 2\pi V/\omega$ is the wave length.

Using relations (4), we obtain the following expressions for the components of displacement of the coating surface:

$$\eta\Big|_{y=0} = \Big(A_1 - i\,\frac{2\pi}{\lambda}\,B_2 \Big)\,\mathrm{e}^{i\omega(x/V-t)}, \qquad \zeta\Big|_{y=0} = \Big(i\,\frac{2\pi}{\lambda}\,B_1 + A_2 \Big)\,\mathrm{e}^{i\omega(x/V-t)}.$$

The compliance is the ratio of strain to applied pressure. The coating compliance has two components: perpendicular to the surface $C_n = |C_n|\,\mathrm{e}^{i\theta_n}$ and parallel to the surface $C_p = |C_p|\,\mathrm{e}^{i\theta_p}$. Here $|C_n|$ and $|C_p|$ are the absolute values of the corresponding components of the dynamic compliance, and θ_n and θ_p are the phase lags of the corresponding components of surface displacement from the acting pressure.

It is convenient to use the following dimensionless complexes for calculations and analysis:

$$C_n^* = \frac{C_n}{H/E} = \frac{\lambda}{H}\Big(\frac{V}{C_t^0}\Big)^2 \frac{2(1+\sigma)\alpha F}{4\pi(1-i\mu)^2[2-(V/C_t^0)^2/(1-i\mu)-2S]},$$

$$C_p^* = \frac{C_p}{H/E} = \frac{\lambda}{H}\,\frac{2(1+\sigma)(S-1)i}{2\pi[2-(V/C_t^0)^2/(1-i\mu)-2S]}.$$

These complexes depend only on the ratio of the wave length to the coating thickness λ/H and on the ratio of the wave velocity to the velocity of propagation of shear perturbations V/C_t^0 in an infinite medium filled by a material with elasticity modulus E without viscous losses ($\mu = 0$). The quantities C_n^* and C_p^* are the ratios of the corresponding components of the dynamic compliance to the static compliance of a bar whose length is substantially greater than its transverse size.

In [2, 3], the complex compliance was calculated for a one-dimensional model of a "locally deformed" coating. It was demonstrated that the dynamic compliance (which contains one component in this case) as a function of

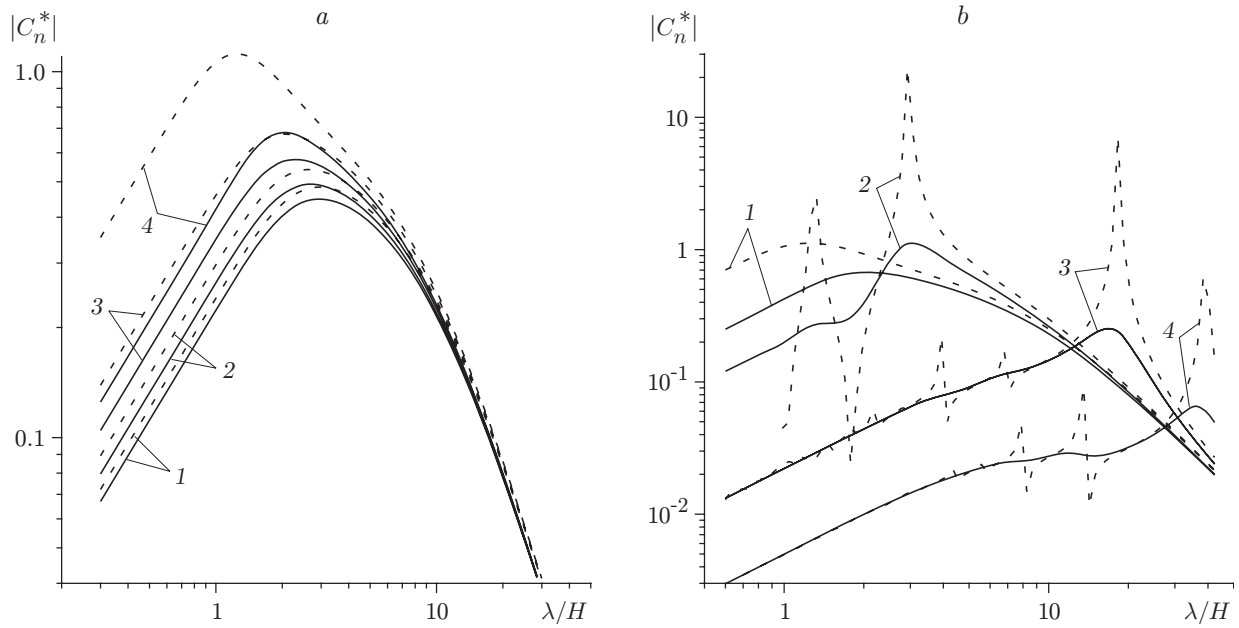

Fig. 1. Dimensionless compliance versus the wave length for $V/C_t^0 < 1$ (a) and $V/C_t^0 > 1$ (b): (a) $V/C_t^0 = 0.1$ (1), 0.5 (2), 0.75 (3), and 0.9 (4); (b) $V/C_t^0 = 1.2$ (1), 1.52 (2), 5 (3), and 10 (4); the solid and dashed curves refer to $\mu = 0.0125$ and 0.4, respectively.

frequency has several minimums and maximums. The value of the first compliance maximum at the frequency of the first resonance

$$f_0 = \sqrt{E/\rho}\,(1+\mu^2)^{1/4}/(4H),$$

rapidly decreases with increasing loss factor. The frequency dependence of the phase shift between strain and pressure changes in a wavelike manner with a period $1/(2f_0)$. The curves become closer to straight lines with increasing viscous losses.

Figure 1 shows the vertical component of the dimensionless compliance as a function of the wave length. For $V/C_t^0 < 1$ (Fig. 1a), all curves have a similar dome-shaped form. The dimensionless compliance increases with increasing wave velocity and decreases with increasing loss factor. The maximum stratification of the curves is observed in the region of the compliance resonance ($\lambda/H = 1$–3). In the long-wave part of the spectrum ($\lambda/H > 10$), the curves corresponding to different values of V/C_t^0 merge together. Nevertheless, there is a small difference between the curves corresponding to different values of μ.

The character of the dependence of the absolute value of the dynamic compliance on the wave length changes when the wave velocity becomes greater than the velocity of propagation of shear oscillations. For $V/C_t^0 \geqslant 1.5$, the value of λ/H that ensures a peak of the dimensionless compliance increases with increasing wave velocity (curves 2–4 in Fig. 1b). The maximum value of the compliance is reached at $V/C_t^0 \simeq 1.52$. The peaks on the compliance curves drastically decrease with increasing viscous losses. For wave lengths several times greater than the wave length at the resonance frequency, the compliance is described by a universal curve whose shape depends neither on wave velocity nor on viscous losses.

The velocity of free strain waves in a layer of a viscoelastic material was calculated in [4]. The maximum amplitude of the vertical component of the traveling strain wave (the resonance peak η/ζ of the first mode of free oscillations) is observed at $V/C_t^0 \simeq 1.52$ [4, Fig. 3b, curve 1]. Thereby, we have $\lambda \simeq 3H$, which agrees well with the results of the present work.

The profiles of the vertical and horizontal displacements characterizing the strain-wave structure were also given in [4]. It was demonstrated that the vertical displacement at the resonance frequency of the first mode of free oscillations [4, Fig. 4a, curve 1] smoothly increases across the coating and reaches a maximum at the outer boundary.

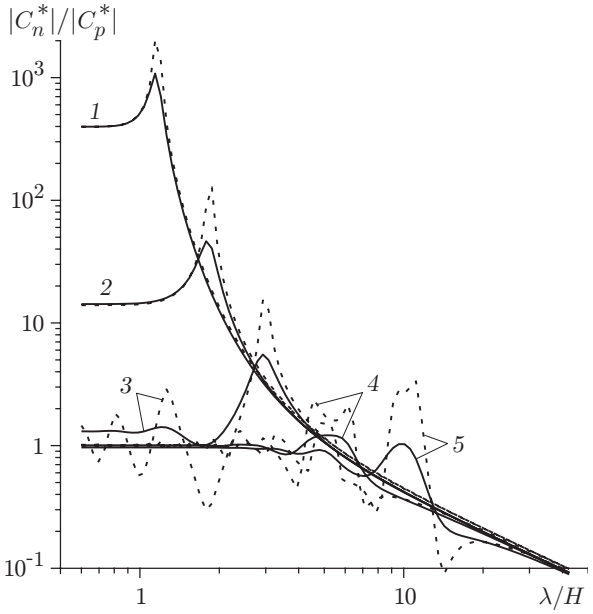

Fig. 2. Ratio of the compliance components versus the wave length for $V/C_t^0 = 0.1$ (1), 0.5 (2), 1.52 (3), 5 (4), and 10 (5): the solid and dashed curves refer to $\mu = 0.0125$ and 0.4.

For $V/C_t^0 > 1.5$ and wave lengths smaller than the wave length at the resonance frequency, Fig. 1b displays additional maximums and minimums located to the left of the peak value on curves 2–4. These peaks arise at the resonance (or anti-resonance) frequencies at which an odd (or, respectively, even) number of maximums of displacements from the equilibrium position fall across the layer. The amplitude of these peaks decreases with increasing resonance multiplicity (mode number) and loss factor of the coating material.

The compliance curves for the horizontal displacement behave similarly. Figure 2 shows the ratio of the absolute values of the vertical and horizontal compliance $|C_n|/|C_p|$, equal to the ratio of the corresponding amplitudes of displacement components $|\eta/\zeta|$, versus the wave length. As the wave velocity decreases, the curves corresponding to this dependence are shifted toward higher values of $|\eta/\zeta|$ and lower wave lengths. For short low-velocity waves, the ratio $|C_n|/|C_p|$ can reach high values (for instance, $|C_n|/|C_p| \simeq 2000$ for $V/C_t^0 = 0.1$ and $\lambda/H \simeq 1.2$). For $\lambda/H > 6$ and $V/C_t^0 > 1.5$, the longitudinal displacements exceed the transverse displacements. Owing to the increase in wave velocity and losses in the material, the longitudinal and transverse strains become closer to each other. The loss factor exerts the most significant effect in the region of the resonance peak of the compliance ratio.

Figure 3 shows the phase lag of the vertical displacement from pressure. For $V/C_t^0 \leqslant 0.5$ (Fig. 3a), the phase angle is mainly determined by the loss factor and depends only weakly on the wave length and its velocity. For $V/C_t^0 > 1.5$ (Fig. 3b), the phase changes by 180° in passing through each resonance. As the loss factor increases, the curves become smoother; the phase increases in the long-wave part of the spectrum and decreases in the short-wave part of the spectrum.

The phase shift between the vertical and longitudinal oscillations also behaves differently in regions located below and above the principal resonance of the coating. Thus, for $V/C_t^0 \leqslant 1.5$ (Fig. 4a), the phase shift varies within 180° with increasing frequency (decreasing λ). For a greater wave velocity (Fig. 4b), a 180° change in the phase shift occurs repeatedly for materials with small losses. These oscillations level off with increasing loss factor.

Figure 5 shows the dependences of max $|C_n^*|$ and λ/H on V/C_t^0 for different values of the loss factor. For low velocities of the wave (low frequency of oscillations, because $f = V/\lambda$), the maximum compliance is independent of the frequency (wave length) and loss factor. For rubber-like materials with $\sigma = 0.5$, the maximum value of the quasi-equilibrium compliance is $|C_n^0| \simeq 0.45H/E$, which is almost twice smaller than the compliance of a bar under static deformation ($f = 0$) under the condition that the bar length is substantially greater than its transverse size.

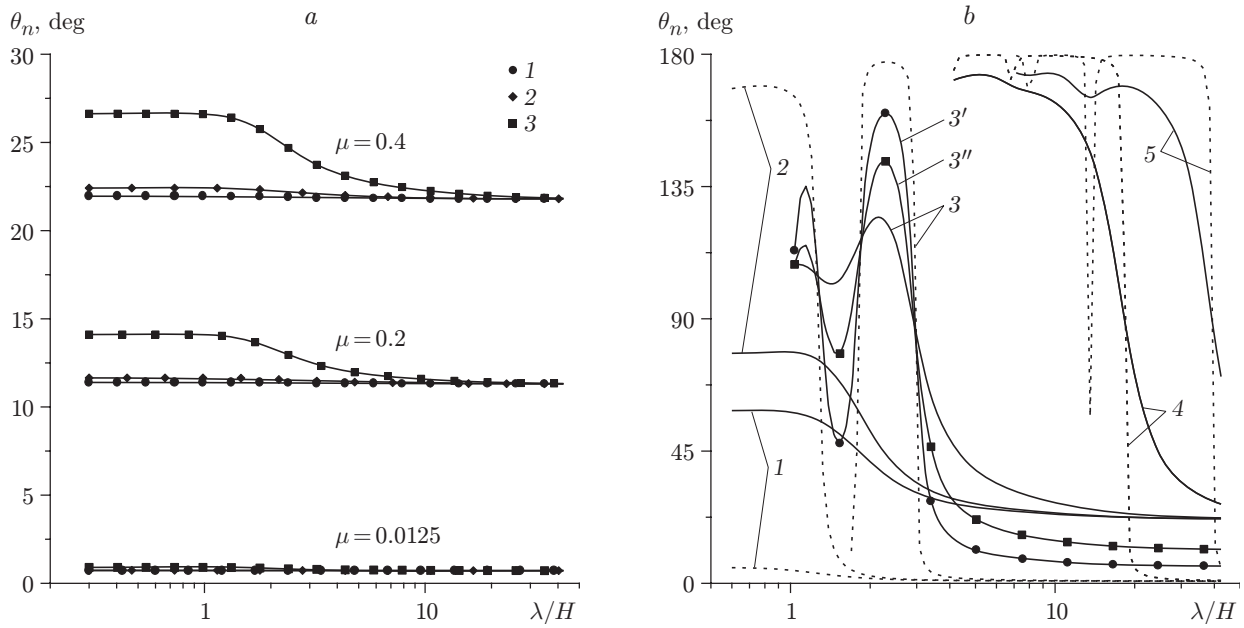

Fig. 3. Phase lag of the vertical displacement from pressure for $V/C_t^0 \leqslant 0.5$ (a) and $V/C_t^0 > 0.5$ (b): (a) $V/C_t^0 = 0.1$ (1), 0.2 (2), and 0.5 (3); (b) $V/C_t^0 = 0.9$ (1), 1 (2), 1.52 (3), 5 (4), and 10 (5); the solid and dashed curves 1–3 refer to $\mu = 0.0125$ and 0.4, respectively; curves 3′ and 3″ refer to $\mu = 0.1$ and 0.2, respectively.

The dynamic response factor $K_d = |C_n|/|C_n^0|$ is a function of the wave length (frequency) and decreases with increasing losses. Thus, the maximum value is $K_d = 19$ for $\mu = 0.05$ and $K_d = 2.5$ for $\mu = 0.4$.

The wave length that ensures the maximum compliance depends weakly on the loss factor (Fig. 5b). The difference arises in the region $0.5 < V/C_t^0 < 1.2$, where the wave length becomes almost one third ($\lambda \simeq H$) of its value in the quasi-equilibrium region, as the loss factor decreases. For $V/C_t^0 > 1$, the wave length that ensures the maximum compliance increases in proportion to the wave velocity.

Figure 6 shows the maximum compliance of the coating in the vertical direction for $\mu = 0.1$ and different values of Poisson's ratio. As the medium compressibility increases (Poisson's ratio decreases), the dimensionless compliance increases, which is particularly noticeable for $\lambda/H > 3$ (Fig. 6a). The condition of resonance $\lambda/H \simeq 3$ for $V/C_t^0 < 1$ is valid only for small values of compressibility. Thus, curve 2 has a weakly expressed resonance character, whereas curves 4 and 5 for $\lambda/H > 5$ asymptotically reach a horizontal line.

The character of the compliance curves changes if the wave velocity exceeds a critical value determined by the expression

$$\frac{V}{C_t^0} = \sqrt{\frac{2(1-\sigma)}{1-2\sigma}}. \tag{5}$$

For $V/C_t^0 = 1.5$, the wave velocity is still insufficient for condition (5) to be satisfied in the indicated range of σ. The compliance peak in Fig. 6b is shifted toward greater wave lengths with decreasing σ.

For curve 2–5 in Fig. 6c, the wave velocity exceeds the critical value determined by condition (5). As in Fig. 6b, with decreasing σ, the maximums of these curves increase and are shifted toward higher wave lengths. In contrast to Fig. 6b, the maximums of the curves are located to the left of the maximum of curve 1, because the curve of the wave velocity versus frequency becomes discontinuous at $\sigma \neq 0.5$ and is shifted toward higher frequencies (lower wave lengths) if the wave velocity becomes greater than the critical value determined by condition (5) (see [4, Fig. 1]).

A method for measuring the vertical component of the compliance of viscoelastic coatings is proposed in [5, 6], and some measured results are given. The compliance measured in experiments should be further compared with data calculated by formulas of the present paper with allowance for measured viscoelastic properties of the material.

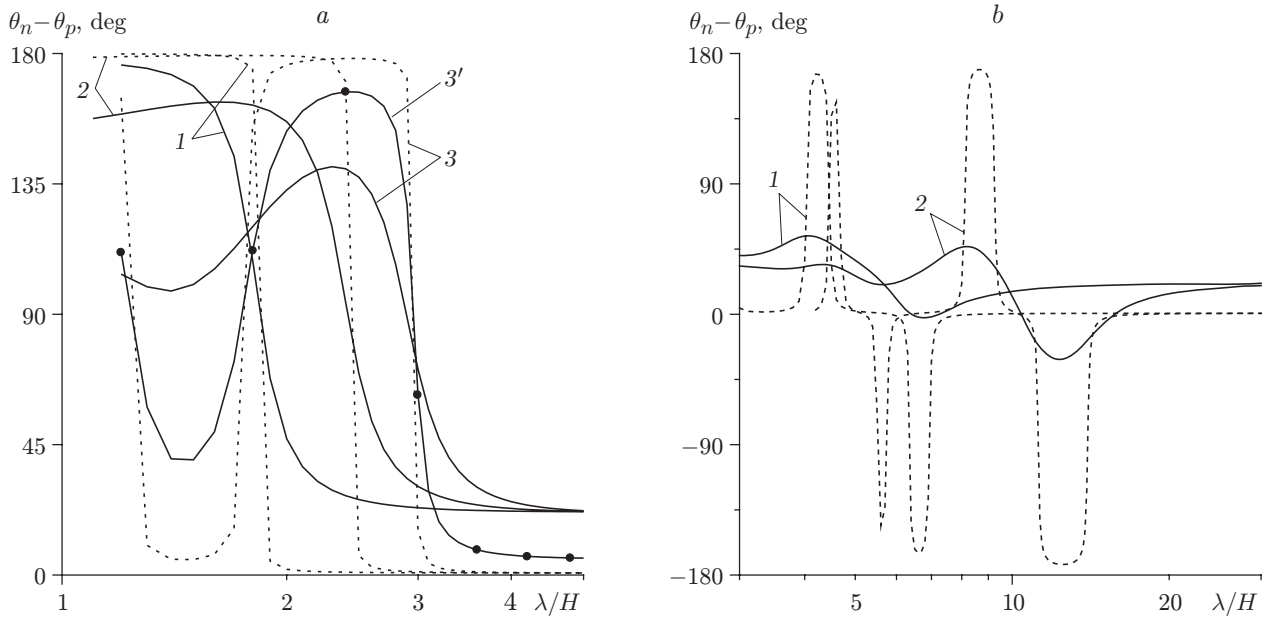

Fig. 4. Phase shift between the vertical and horizontal displacements for $V/C_t^0 \leqslant 1.5$ (a) and $V/C_t^0 > 1.5$ (b): (a) $V/C_t^0 = 0.5$ (1), 1 (2), and 1.5 (3); the solid and dashed curves refer to $\mu = 0.0125$ and 0.4, respectively; curve 3′ refers to $\mu = 0.2$; (b) $V/C_t^0 = 5$ (1) and 10 (2); the solid and dashed curves refer to $\mu = 0.025$ and 0.4, respectively.

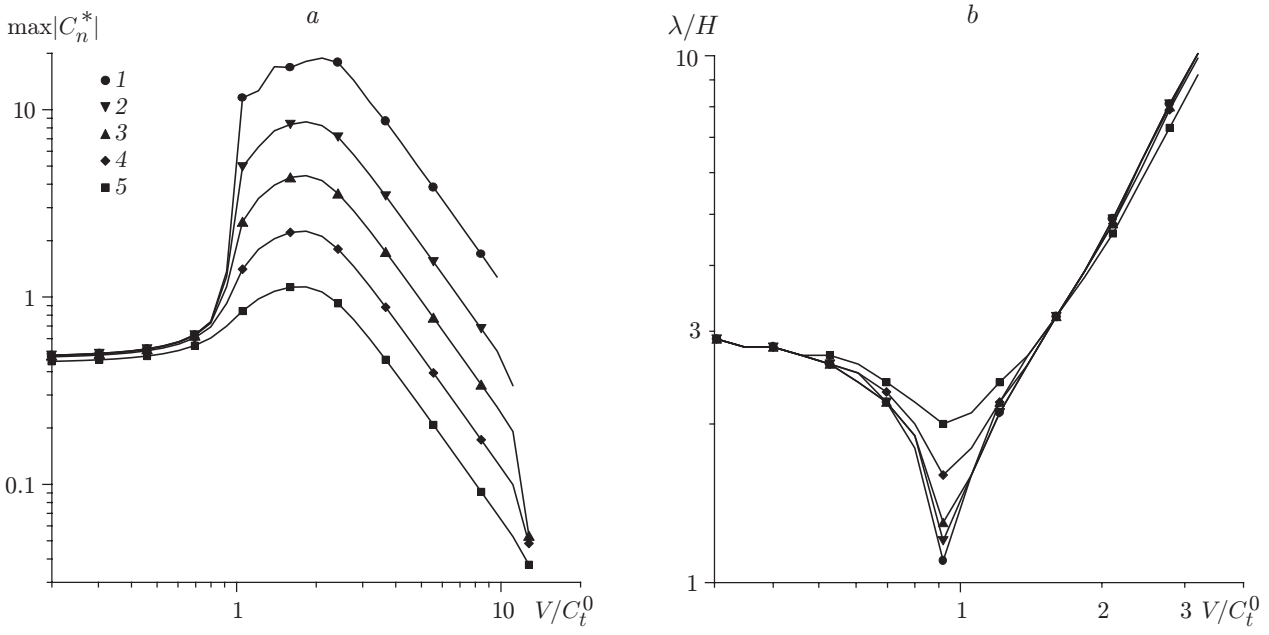

Fig. 5. Dependences of max $|C_n^*|$ (a) and λ/H (b) versus V/C_t^0 for different values of the loss factor ($\sigma = 0.5$): $\mu = 0.02$ (1), 0.05 (2), 0.1 (3), 0.2 (4), and 0.4 (5).

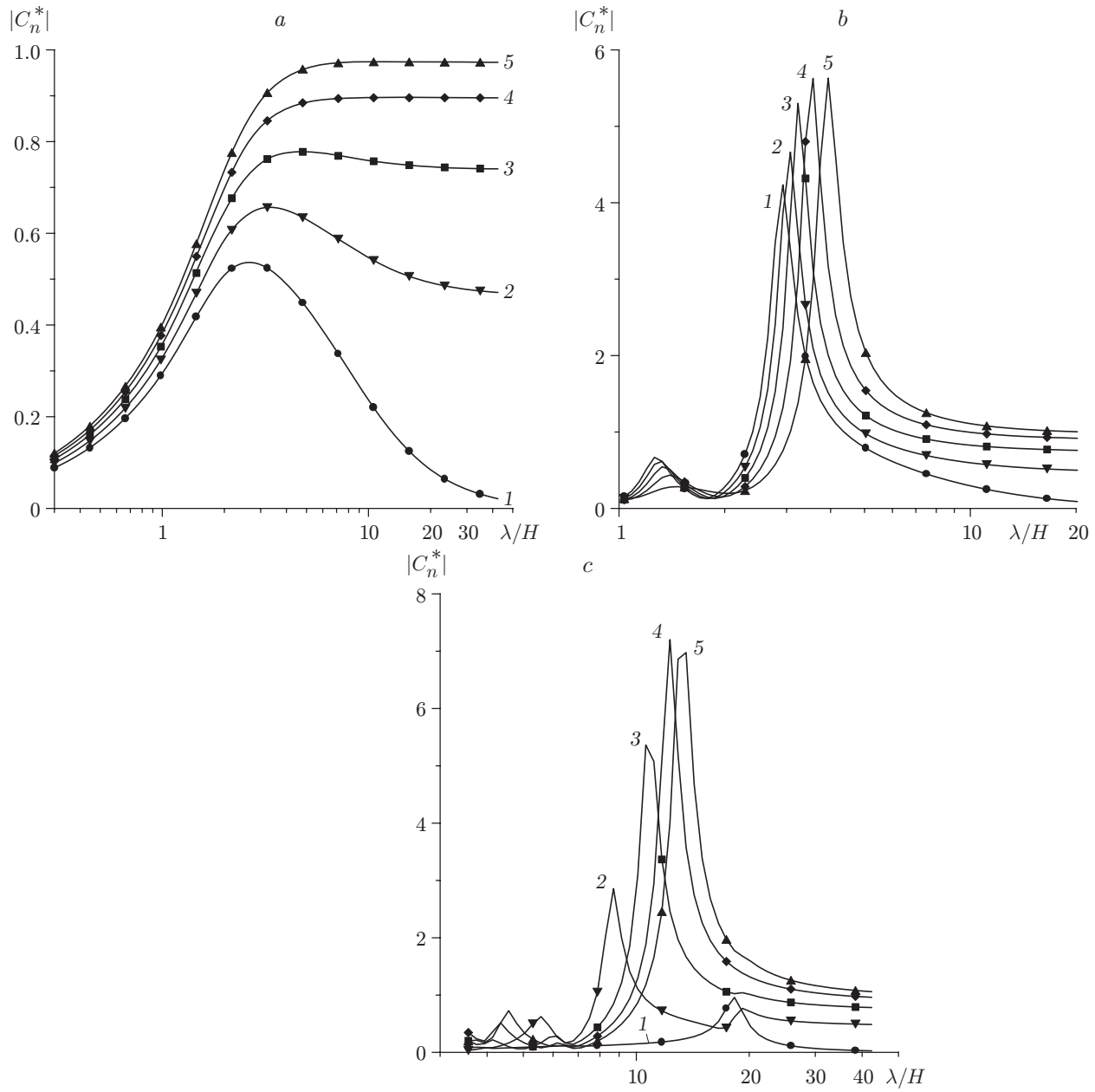

Fig. 6. Dimensionless compliance versus the wave length for $V/C_t^0 = 0.5$ (a), 1.5 (b), and 5 (c) and different Poisson's ratios ($\mu = 0.1$): $\sigma = 0.5$ (1), 0.4 (2), 0.3 (3), 0.2 (4), and 0.1 (5).

It follows from the results obtained in the present work that the compliance of a viscoelastic coating depends not only on the frequency but also on the length of the pressure wave. The longitudinal strain under certain conditions is demonstrated to be rather high and even to exceed the vertical strain. These facts should be taken into account in explaining the mechanism of drag reduction by the presence of compliant coatings in a turbulent flow, determined by correlation of longitudinal and vertical perturbations introduced by the coating into the near-wall flow region. Therefore, phase relations between these perturbations are also important. Compliant coatings made of a material with Poisson's ratio $\sigma \neq 0.5$ (e.g., polyurethane foam) seem to be the most efficient ones, because they have greater compliance at low velocities.

REFERENCES

1. L. D. Landau and E. M. Lifshits, *Theory of Elasticity, Pergamon Press*, Oxford–New York (1970).
2. B. N. Semenov, "Analysis of strain characteristics of viscoelastic coatings," in: B. P. Mironov (ed.), *Hydrodynamics and Acoustics of Near-Wall and Free Flows* (collected scientific papers) [in Russian], Inst. Thermophys., Sib. Div., Acad. of Sci. of the USSR, Novosibirsk (1981), pp. 57–76.
3. B. N. Semenov, "Analysis of four types of viscoelastic coatings for turbulent drag reduction," in: *Emerging Techniques in Drag Reduction*, MEP, London and Bury St. Edmunds (1996), pp. 187–206.
4. V. M. Kulik, "Plane strain wave in an isotropic layer of a viscoelastic material," *J. Appl. Mech. Tech. Phys.*, **47**, No. 3, 394–400 (2006).
5. V. M. Kulik, S. L. Morozova, and S. V. Rodyakin, "Measurement of the complex compliance of coatings of elastic materials," *J. Eng. Phys. Thermophys.*, **75**, No. 2, 401–405 (2002).
6. V. M. Kulik, S. V. Rodyakin, I. Lee, and H. H. Chun, "Deformation of a viscoelastic coating under the action of convective pressure fluctuations," *Exp. Fluids*, **38**, No. 5, 648–655 (2005).